International Journal of Science and Research (IJSR)
ISSN: 2319-7064
ResearchGate Impact Factor (2018): 0.28 | SJIF (2018): 7.426

Power Sharing Strategy in Islanded Microgrids

Xuan Hoa Thi Pham

Department of Electrical and Electronic Engineering, University of Food Industry, Ho Chi Minh City, Vietnam

Abstract: ***This paper presents a power sharing control method for use between paralleled three-phase inverters in an islanded microgrid under unbalanced and non-linaer loads. In this study, the mismatch of power sharing when the line impedances have significant differences for inverters connected to a microgrid has been solved, the accuracy of power sharing and voltage quality in an islanded microgrid are improved, the voltage droop slope is tuned to compensate for the mismatch in the voltage drops across line impedances by using communication links. The method will ensure in accurate power sharing even if the communication is interrupted. If the load changes while the communication is interrupted, the accuracy of power sharing is reduced but the proposed method is better than the conventional droop control method. In addition, the accuracy of power sharing base on the proposed methodis not affected by the time delay in the communication channel and local loads. The control model has been simulated in Matlab/Simulink with two or three inverters are connected in parallel. The simulation results demonstrate the accuracy of the proposed control method. Futhermore, in order to validate the theory analysis and simulation results, the experimental setup was built in laboratory and the experimental results have demonstrated the effectiveness of proposed methods.***

Keywords: Droop control, power sharing, microgrid control, parallel inverter, voltage, line impedance, voltage unbalanced compensation

1. Introduction

In the microgrid, inverters are connected in parallel to form a backup system, improve the reliability, reduce the overload of each inverter, and provide flexibility. However, when a microgrid is operating in the islanded mode, each of the inverter should be able to supply its share of the total load in proportion to its rating. The control strategies for this mode are usually divided into two main types [1], [2] as follows. The first type is made up of the communication-based control techniques including concentrated control, master/slave control and distributed control. These techniques can achieve an excellent proper power sharing. However, these control strategies required communication lines between the modules which may increase cost of systems. Long distance communication lines are easier to disrupt, which reduces system reliability and expandability. The second type is based on the droop control technique without requiring communications, and it is widely used in conventional power systems [2]-[3], [4], [5]-[7]. The reason for the popularity of this droop control technique is that it provides a decentralized control capability that does not depend on external communication links. These techniques enable the "plug-and-play" interface and enhance the reliability of systems. However, communications can be used in addition to the droop control method to enhance the system performance without reducing reliability [8]-[18].

Traditional droop control techniques have some disadvantages in the power sharing due to the following reasons:

- The line impedances are not available and different from each other. This has a significant effect on power sharing due to different voltage drops. When the impedances of the lines connecting inverters to the common connection point are different, a current imbalance appears when the load sharing error increases [1].
- The heterogeneous line impedance, including the resistor and capacitance, is not suitable for conventional droop control with pure resistors or pure capacitance applying for the low voltage distribution [1], [18]. Moreover, with a heterogeneous line impedance, the active and reactive power interact with each other, which leads to difficulty for separate control [1]. Although frequency droop techniques can achieve accurate real power sharing, they typically result in poor reactive power sharing due to mismatches in the impedances of the DG unit feeders and the different ratings of the DG (distributed generation) units [7]-[13]. Consequently, the problem of reactive power sharing in islanded microgrids has received considerable attention in the literature and many control techniques have been developed to address this issue [16]-[18]. Currently, the studies for power sharing between inverters have the following disadvantages:
- Communication links are used in some droop improvement studies to enhance the accuracy of power sharing, but the implementation of this technique is sensitive to communication delays, delays in delivery can further reduce the accuracy of the power sharing [12-15].
- The reliability of these studies are also affected when the communication is interrupted [16-18].
- Improved power sharing methods can reduce the quality of the voltage, such as: virtual output impedance method [19].
- The accuracy of power sharing is enhanced negligible if local loads are connected at the output of each inverter [20].

Another problem in islanded microgrids is that they must harmonics power sharing between inverters when microgrid has nonlinear loads and unbalanced loads are connected. In fact, thew conventional droop controllers are designed to share fundamental positive-sequence power components. Therefore, some studies have applied control methods to reduce distortion due to harmonics and to control harmonics between DG units. For example, the virtual output impedance method is introduced to automatically share the harmonic currents [19,6,18,4] between the DG units. This method, in order to reduce the effect of mismatch of the line impedances in power sharing, a large virtual impedance value is designed. As a result, the more voltage distortions exist. Another approach, uses a virtual capacitive loop to improve the voltage distortion and to share accurately the harmonic current [23,24] However, this method is based on knowing the line impedances to adjust the appropriate virtual impedance value.

In [25,26], the authors propose a harmonic droop controller to reduce the voltage harmonics distortion at the PCC and to share harmonics between the inverters. However, this method is complicated. Furthermore, in a low voltage (LV) microgrid, the total harmonic distortion (THD) is highly affected by the line impedances in the microgrid.

This paper proposes a method to compensate for the mismatch in the voltage drops across line impedances, proposed method allows an accurate power sharing ratio between the parallel inverters in islanded microgrids without being affected by:

- The line impedances have significant differences for inverters connected to point of common coupling (PCC).
- Microgrid have the local loads at the output of inverters.
- Mitigate the voltage harmonic distortion generated by non-linear loads.
- The communication is interupted or delay.

2. Islanded Microgrid Control

a) The proposed control method

The structure of an islanded microgrid is made up of many inverters connected in parallel. In Figure 1, a block diagram of inverters is provided. Each inverter is connected to a common bus at the PCC through the line impedance. In addition, the loads of the microgrd are also connected to the common bus. The proposed controller contains two control loops, where the outer loop power control divides the capacity of each inverter and the inner loop control makes the voltage and current output of the inverters similar to the references. The voltage magnitude signal from the PCC are provided by a low-bandwidth connection. The inner loops are the current and voltage control to adjust the current and voltage at the inverter output.

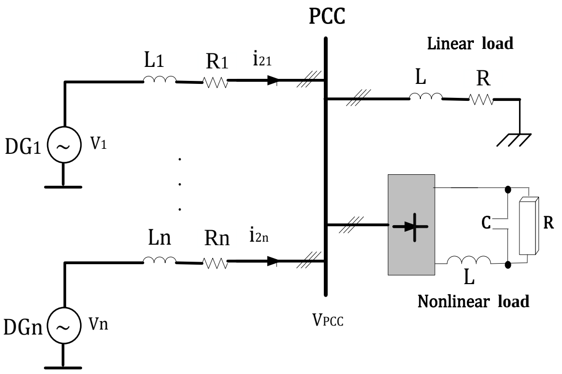

Figure 1: A block diagram of inverters in islanded microgrid

1) The principle of the proposed control method

The principle of the droop control method is explained by considering the equivalent circuit of an inverter connected to an AC bus. The analysis method is based on Thevenin theorem as shown in Figure 2.

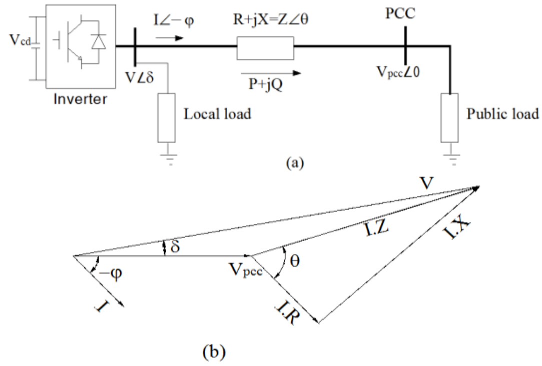

Figure 2: (a) Equivalent schematic of inverters connected to a load; (b) vector diagram of voltage and current.

The active and reactive power supplied by the inverter are calculated as follows:

$$P = \frac{V}{R^2 + X^2}[R(V - V_{PCC}\cos\delta) + XV_{PCC}\sin\delta] \quad (1)$$

$$Q = \frac{V}{R^2 + X^2}[-RV_{PCC}\sin\delta + X(V - V_{PCC}\cos\delta)] \quad (2)$$

In general, both the inductance X and resistor R are considered. The use of an orthogonal linear rotational transformation matrix T from active power P and reactive power Q to active power P’ and reactive power Q’ is determined by:

$$\begin{bmatrix} P' \\ Q' \end{bmatrix} = [T]\begin{bmatrix} P \\ Q \end{bmatrix} = \begin{bmatrix} \frac{X}{Z}P - \frac{R}{Z}Q \\ \frac{R}{Z}P + \frac{X}{Z}Q \end{bmatrix} \quad (3)$$

When the power angle δ is small, equations (1), (2) and (3) can be rewritten as:

$$\delta \cong \frac{ZP'}{VV_{PCC}};\ V - V_{PCC} \cong \frac{ZQ'}{V} \quad (4)$$

From (4), the basis of the well-known frequency andvoltage droop regulation through active and reactive power is calculated by:

$$\omega = \omega_0 - m_p P' \quad (5)$$

$$V = V_0 - m_q Q' \quad (6)$$

where V_0 and ω_0 are the nominal amplitude voltage and frequency of the inverter, respectively; V_S and ω are the measured amplitude voltage and frequency of the inverter, respectively; and m_p and m_q are the active and reactive droop coefficients, which are calculated as follows:

$$m_p = \frac{\omega_0 - \omega_{min}}{P_{max}};\ m_q = \frac{V_0 - V_{min}}{Q_{max}} \quad (7)$$

The impedance of the lines connecting the inverters to the PCCis significantly different, the load sharing accuracy is difficult to achieve and voltage adjustment is difficult because it depends on the parameters of the system. From (5) and (6), the following are obtained:

$$m_{q1}Q_1' = m_{q2}Q_2' = \cdots = m_{qn}Q_n' = \Delta V_{max} \quad (8)$$

$$m_{p1}P_1' = m_{p2}P_2' = \cdots = m_{pn}P_n' = \Delta\omega_{max} \quad (9)$$

Combining the equations (1), (2), (3), (5), (6), (8) and (9), produces the conditions for accurately rated power sharing as in (10):

$$\begin{cases} \frac{m_{p1}}{m_{p2}} = \frac{Z_1}{Z_2} \\ \delta_1 = \delta_2 \\ V_1 = V_2 \\ \frac{m_{q1}}{m_{q2}} = \frac{Z_1}{Z_2} \end{cases} \qquad (10)$$

To satisfy (10), it is necessary to choose droop coefficients that are proportional to the line impedance. If the system is adjusted to meet the requirements, the droop affects the quality of the frequency and voltage. Therefore, a controller is proposed to ensure the accurate power sharing of parallel inverters. The proposed controller is shown in Figure 3.

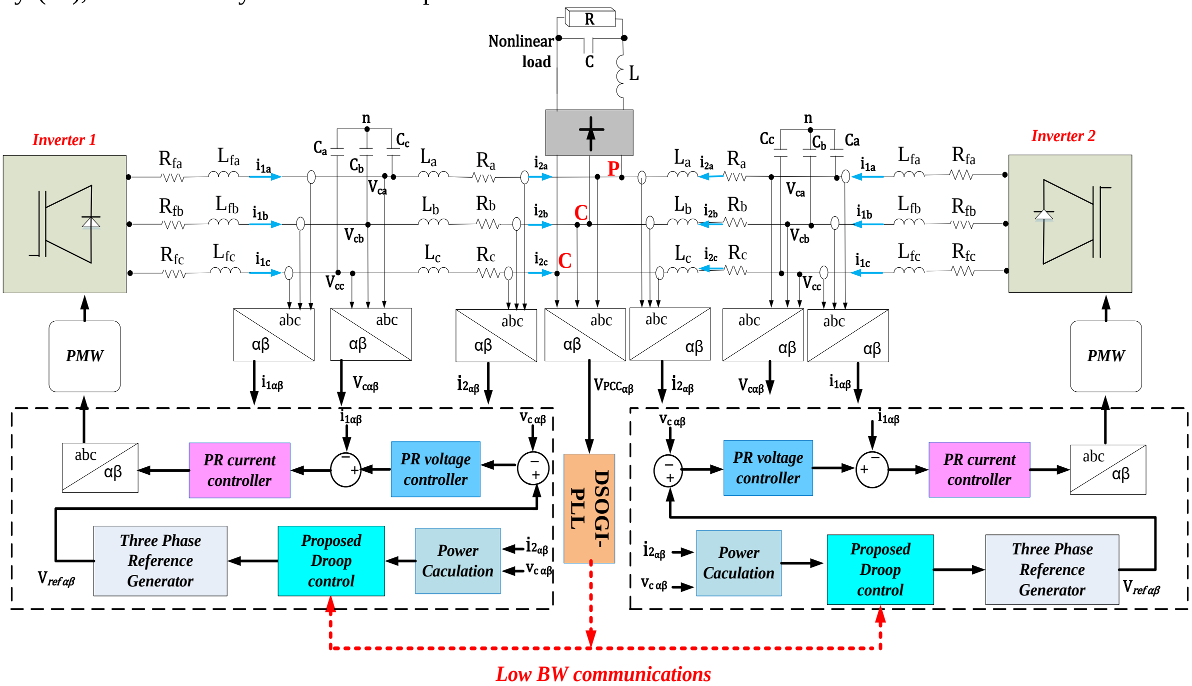

Figure 3: Block diagram of the proposed controller for islanded microgrid

The proposed controller consists of the following main blocks:

2) Calculation of active power and reactive power

The active and reactive power produced by converters are calculated in a stationary $\alpha\beta$ frame:

$$p = \frac{3}{2}(i_{2\alpha}v_{c\alpha} + i_{2\beta}v_{c\beta}) \qquad (11)$$

$$q = \frac{3}{2}(i_{2\alpha}v_{c\beta} - i_{2\beta}v_{c\alpha}) \qquad (12)$$

This paper has used double second order generalized integrator - quadrature signal generation (DSOGI-QSG) for caculation of active power and reactive power. To simplify, although the voltage may contain negative sequence components due to imbalanced load in the system, it is assumed that the negative sequence voltage is relatively small and is ignored. In this case, with the basic fundamental components are detected, the active, reactive and unbalanced powers of the three-phase inverters can be calculated as the Figure 4.

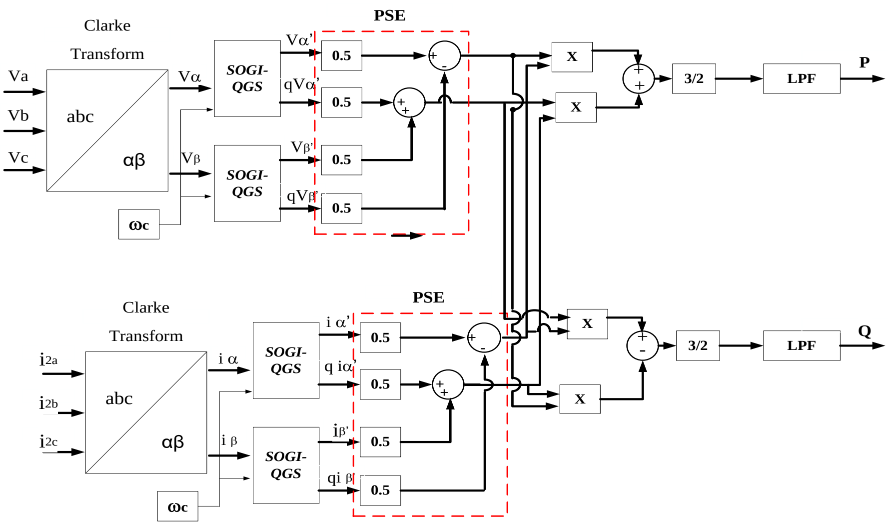

Figure 4: Block diagram of Calculation of active power and reactive power

3) The proposed reactive power sharing controller

In this paper, the voltage droop slope is tuned to compensate for the mismatch in the voltage drops across line impedances by:

$$V_{ref} = k_p \int (V' - V_{PCC})\,dt \qquad (13)$$

Where: V ' is the voltage at the output of the traditional Droop controller, which is determined by the equation (6).

$$V' = V_0 - m_q Q' \qquad (14)$$

Where: k_p is the gain of the integral, V_{pcc} is the voltage at PCC.

4) The proposed active power sharing controller

According to the studies [12] – [22], the line impedance does not affect significantly to the accuracy of the active power sharing, so in this paper uses the traditional Droop controller to active power sharing. The proposed controller to active power sharing and reactive power sharing are shown in Figure 5.

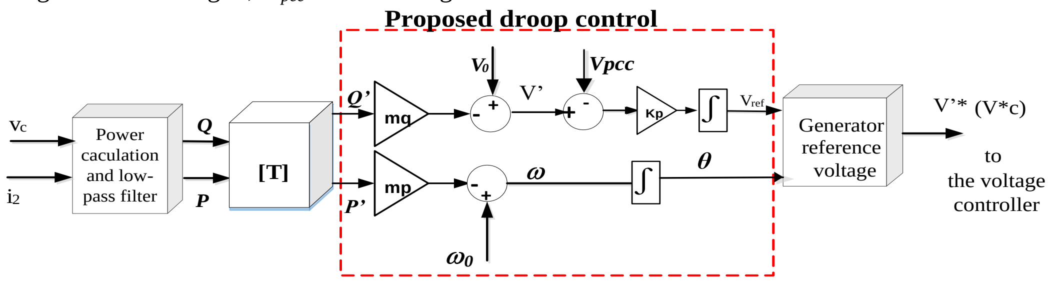

Figure 5: Proposed active power sharing and reactive power sharing control

5) Survey the stability of the control system

From (1), (2), (3) and (4), we can write:

$$P' = \frac{VV_{PCC}\sin(\delta - \delta_{PCC})}{Z} \qquad (15)$$

$$Q' = \frac{V^2 - VV_{PCC}\cos(\delta - \delta_{PCC})}{Z} \qquad (16)$$

Where V_{pcc} are the output of DSOGI-PLL blocks, Vis the output of the reactive power sharing from the controller, and δ is the output of the active power sharing controller.

By linearizing (13), (14) and (16) around Q', V and V_{pcc} the following is obtained:

$$\Delta V_{ref} = k_p \int (\Delta V' - \Delta V_{PCC})\,dt \qquad (17)$$

$$\Delta V' = \Delta V_0 - m_q \Delta Q' \qquad (18)$$

$$\Delta Q' = \frac{\partial Q'}{\partial V}\Delta V + \frac{\partial Q'}{\partial V_{PCC}}\Delta V_{PCC} = A\Delta V + B\Delta V_{PCC} \qquad (19)$$

Where:

$$A = \frac{2V - V_{PCC}\cos(\delta - \delta_{PCC})}{Z}$$

$$B = -\frac{V}{Z}\cos(\delta - \delta_{PCC})$$

The relationships among (17), (18) and (19) are shown in Figure 6.

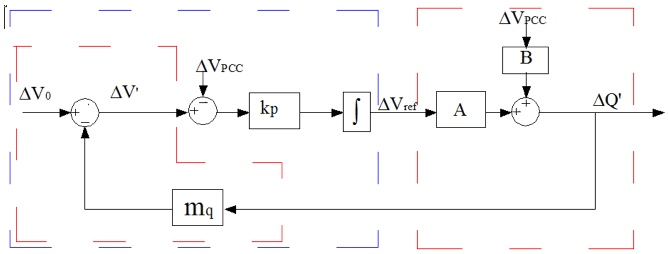

Figure 6: Small signal reactive power sharing droop control.

The transfer function of Figure 5 is as follows:

$$\Delta Q'(S) = \frac{k_p A}{S + k_p.m_q.A}\Delta V_0(S) + \frac{SB - k_p A}{S + k_p.m_q.A}\Delta V_{PCC}(S) \qquad (20)$$

From (20), λ can be calculated as:

$$\lambda = -k_p.m_q.A \qquad (21)$$

The transfer function (20) has shown that the constant of the loops control can be adjusted by k_p, and not by m_q. The reactive power sharing no longer affects the quality of the voltage or frequency.

By linearizing (5) and (15) around P', δ and δ_{pcc} the following is obtained:

$$\Delta\omega = \Delta\omega_0 - m_p \Delta P' \qquad (22)$$

$$\Delta P' = C\Delta\delta + D\Delta\delta_{PCC} \qquad (23)$$

Where:

$$C = \frac{VV_{PCC}\cos(\delta - \delta_{PCC})}{Z}$$

$$D = -\frac{VV_{PCC}}{Z}\cos(\delta - \delta_{PCC})$$

$$\Delta P' = C\Delta\delta + D\Delta\delta_{PCC} = C(\Delta\delta - \Delta\delta_{PCC}) \qquad (24)$$

The relationships among (22) and (24) are shown in Figure 7.

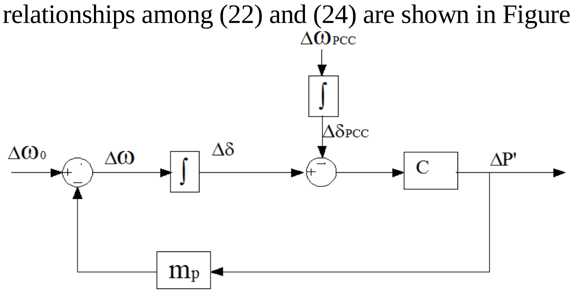

Figure 7: Small signal active power sharing droop control

The transfer function of Figure 7 is as follows:

$$\Delta P'(S) = \frac{C}{S + m_p.C}\Delta\omega_0(S) + \frac{C}{S + m_p.C}\Delta\omega_{PCC}(S) \qquad (25)$$

From (23), λ can be calculated as:

$$\lambda = -m_p.C \qquad (26)$$

m_p is determined by the equation (7).

6) The current and voltage controller

The voltage and current controllers are implemented on the stationary frame and the proportional resonant (PR) controllers are employed in the αβ frame by using the following transfer function.

$$G_V(S) = k_{pv} + \sum_{h=1,3,5,7} \frac{2k_{vh}\omega_c S}{S^2 + 2\omega_c S + (2\pi hf)^2} \quad (27)$$

$$G_i(S) = k_{pi} + \sum_{h=1,3,5,7} \frac{2k_{ih}\omega_c S}{S^2 + 2\omega_c S + (2\pi hf)^2} \quad (28)$$

Where k_{pv} and k_{pi} are the proportional gains, k_{vh} and k_{ih} respectively represent the voltage and current resonant controller coefficients for the h^{th} order harmonic component (including fundamental component as the first harmonic) and ω_c represents cutoff frequency for resonant bandwidth control.

7) Modeling of a three phase DSOGI-PLL

Figure 8 shows the structure of a DSOGI-PLL. Both of the adaptive filtering technique and the in-quadrature phase detection technique are used in the DSOGI-PLL to generate the frequency and phase outputs. This system has a double feedback loop, i.e. the frequency/phase generator provides both the phase-angle to the Park transform and the central frequency to the second order-generalized integrator - quadrature signal generation (DSOGI-QSG) [25].

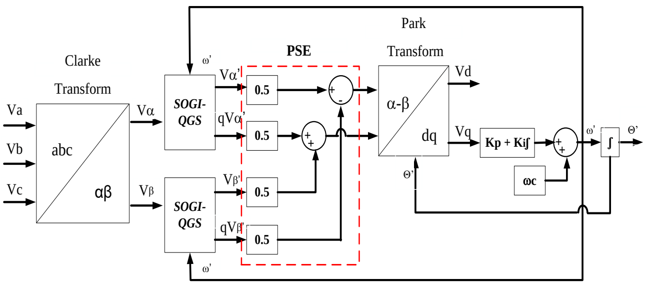

Figure 8: Modelling of a three phase DSOGI-PLL

The parameters of the DSOGI-PLL are chosen as follows: $k=\sqrt{2}$, t_s=100ms, $\varepsilon = 1/\sqrt{2}$ and $T_i = t_s s^2/2.3 = 0.021\,s$. Figure 9 shows the responses of the DSOGI-PLL.

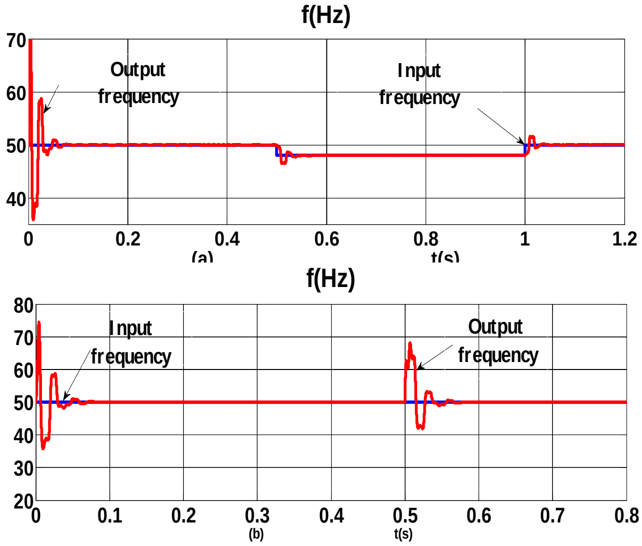

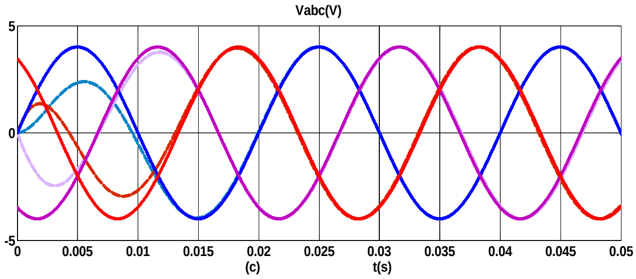

Figure 9: Responses of a DSOGI-PLL.

Figure 9(a) shows the frequency response of a DSOGI-PLL when the frequency of the input signal changes from 50Hz to 48Hz at t = 0.5s, and from 48Hz to 50Hz at t=1s. Figure 9(b) shows the frequency response of a DSOGI-PLL when the phase angle of the input signal changes from 0° to 45° at t=0.5s. Figure 9(c) shows the response of the input and output voltages of a DSOGI-PLL. The simulation results in Figure 9 show that the DSOGI-PLL can obtain the exact voltage amplitude and frequency at the point of common coupling (PCC). The voltage amplitude is the input for the inner-controller. Therefore, when more exact values are obtained, more accurate power sharing is achieved.

b) Analyze the effect of local loads on reactive power sharing

The active power sharing base on frequency droop is not affected by the local loads. However, the local loads will affect the reactive power sharing during islanding operation [15-25], is showed in figure 10.

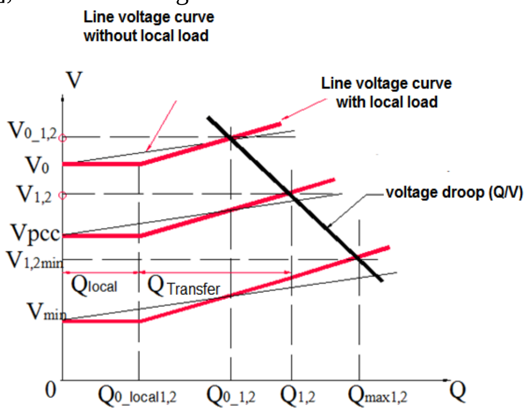

Figure 10: Reactive power flows of two inverters with local loads and line impedances are the same

The Figure 10 shows:

When the microgrid has not local loads, slope $k_{q1,2}$:

$$k_{q1,2} = \frac{V_{0\_12} - V_0}{Q_{0\ 12}} \quad (29)$$

When the microgrid has local loads, slope k_q:

$$k_{q1,2} = \frac{V_{0\_12} - V_0}{Q_{0\ 12} - Q_{0\ local12}} \quad (30)$$

Where:

V_0: the nominal amplitude voltage at the PCC

$V_{0\_1,2}$: the nominal amplitude voltage of inverters 1, 2.

$Q_{0\_1,2}$: the nominal reactive power of inverters 1, 2.

$Q_{0\_cục\ bộ1,2}$: the nominal reactive power of local loads 1, 2.

In the case of the different local loads or different inverters will lead to reactive power sharing is inaccuracy, as shown in Figure 11 and 12.

International Journal of Science and Research (IJSR)
ISSN: 2319-7064
ResearchGate Impact Factor (2018): 0.28 | SJIF (2018): 7.426

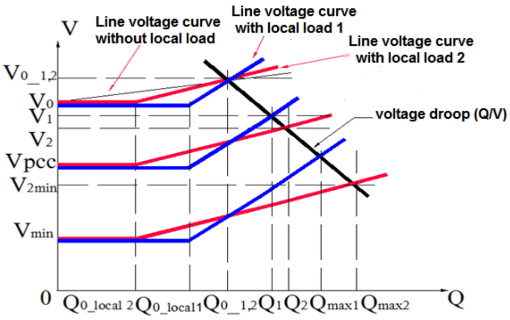

Figure 11: Reactive power flows of two inverters with local loads are diffirence

When the microgrid has local load 1, slope k_{q1}:

$$k_{q1} = \frac{V_{0\_1,2} - V_0}{Q_{0\_1,2} - Q_{0\_local1}} \tag{31}$$

When the microgrid has local load 2, slope k_{q2}:

$$k_{q2} = \frac{V_{0\_12} - V_0}{Q_{0\_1,2} - Q_{0\_local2}} \tag{32}$$

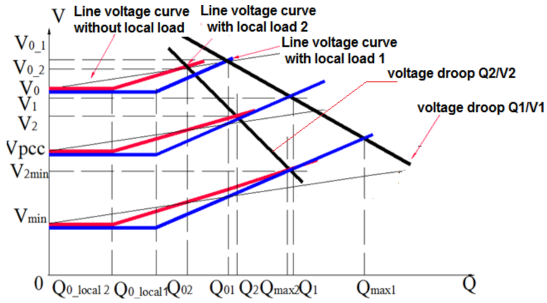

Figure 12: Reactive power flows of two inverters and local loads are diffirence

When the microgrid has local load 1, slope k_{q1}:

$$k_{q1} = \frac{V_{0\_1} - V_0}{Q_{0\_1} - Q_{0\_local1}} \tag{33}$$

When the microgrid has local load 2, slope k_{q1}:

$$k_{q2} = \frac{V_{0\_2} - V_0}{Q_{0\_2} - Q_{0\_local2}} \tag{34}$$

Figure 10, 11 and 12 shown that when microgrid has local loads at the output of the inverters, the local loads will make to change the output voltage of the inverters, the voltage of the local loads are equal with the voltage at the PCC. Therefore, the local loads make an offset in the output voltage of the inverters, this is also the cause of mismatch for reactive power sharing in islanded microgrid.

By adjusting the integral gain coefficients $k_p$for the proposed controllers at the equation (13), when it is in the set state, the voltages V' of inverters will come to an equal voltage ($V'_1 = V'_2 = \ldots V'_n = V_{PCC}$). This means that the deviation of the voltage drop across the line and the difference of the local loads are eliminated. In other words, the effect of the deviation of the line impedance and the difference of local loads are eliminated. As a result, if inverters are the same, local loads and line impedance are the same or different, the power sharing for each inverter is:

$$P_1 = P_2 = P_n = \frac{1}{n}\left(P_{public} + P_{local\ 1} + P_{local\ 2} + \cdots + P_{local\ n}\right) \tag{35}$$

$$Q_1 = Q_2 = Q_n = \frac{1}{n}\left(Q_{public} + Q_{local\ 1} + Q_{local\ 2} + \cdots + Q_{local\ n}\right) \tag{36}$$

c) The improve proposed controller

Proposed droop controller in Figure 5 was added to the block composed of logic gates in order to improve reliability for the controller in case of communication is interrupted. The time out/enable logic is shown in figure 13.

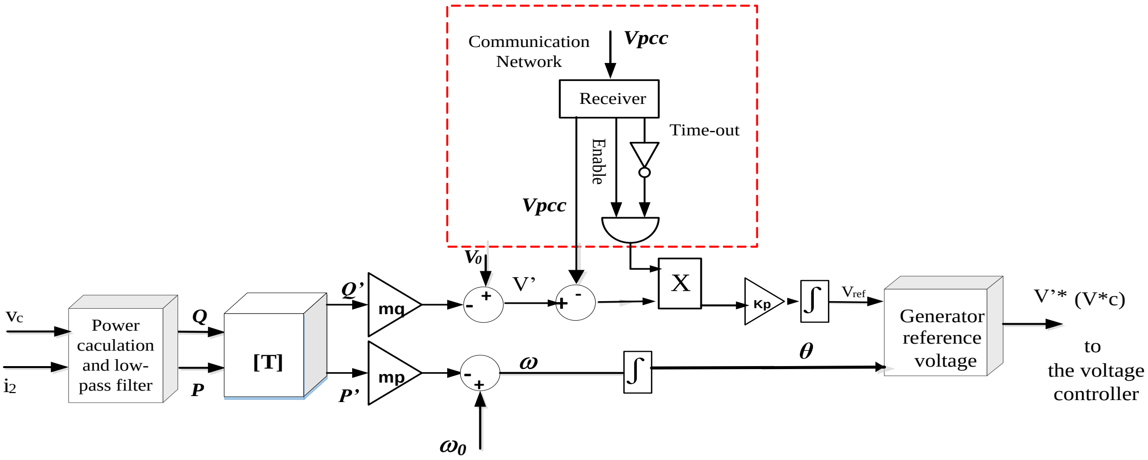

Figure 13: Proposed active power sharing and reactive power sharing control is improved

When the communication is interrupted, in which case the control loop is disabled and the integrator output will remain constant until the communication is restored. The amplitude voltage at output of proposed adaptive droop are held at the last value before the communication failure occurred due to the integral action of the controller. The power sharing is still accurate if the operating point remains unchanged after the communication failure, but if the load changes the power sharing error is still acceptable.

The time delay is called the information update delay. The proposed droop controller is immune to the time delay in the communication channel. Communication link only used to set the value of the reference voltage for tuning the output voltage of the controller. Moreover, the reference voltage is the amplitude value therefore the system will reach steady state despite is slower than usual. If delays occur in steady state, it will not affect the power sharing accuracy. The reference voltage depends on the load so it is a fixed reference voltage until the load changes. Therefore, the accurate power sharing at steady state is unaffected by time delays in the communication channels.

3. Simulation Results and Discussion

A microgrid with two or three parallel inverters, as shown in Figure 1, is simulated in Matlab/Simulink. All of the simulation parameters of the system are given in Table I.

Table I: Parameters for the Controllers

Parameters	Values	Parameters	Values
Input source voltage V_{cd} (V)	600	Rate frequency f_0(Hz)	50
Filter inductance L_f(mH)	1.2	Rate power (kVA)	5
Filter resistance R_f(Ω)	0.2	Rate voltage $V_{AC,\,p}$ (V)	310
Filter capacitance C (μF)	50	Droop coefficient m_q(V/Var)	1.7e-3
Switching frequency f_0(kHz)	10	Droop coefficient m_p (rad/s /W)	1e-4
k_{pi}	75	k_{pv}	0.25
k_{ih}	550(h=1) 50(h=5) 40(h=7) 20(h=11)	k_{vh}	15(h=1) 10(h=5,7, 11,13)

a) Simulation for power sharing of two identical inverters, the line impedances are difference

In this case, the line parameters of the two inverters are given in Table II. The simulation results for this case including the real power output, reactive power output, current outputand load voltage are shown in Figure 11.

Parameters of load:
Non-linear load: R_{NL}=200Ω, L_{NL}=200mH, C_{NL}=84μF
Linear load: P=3000W, Q=2800 kVar (t=0-5s)
P=2000W, Q=1800 kVar (t=5-10s)

Table 2: Line Parameters of Two Inverters

Line parameters	Inverter 1	Inverter 2
Resistance R (Ω)	0.8	1
Inductance L (mH)	0.6	0.9

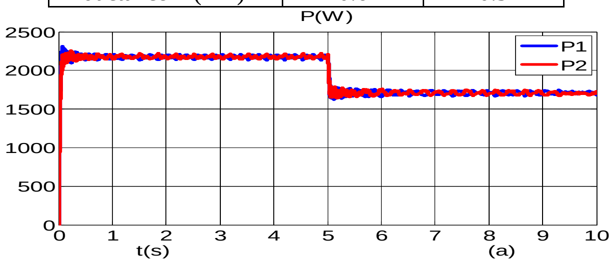

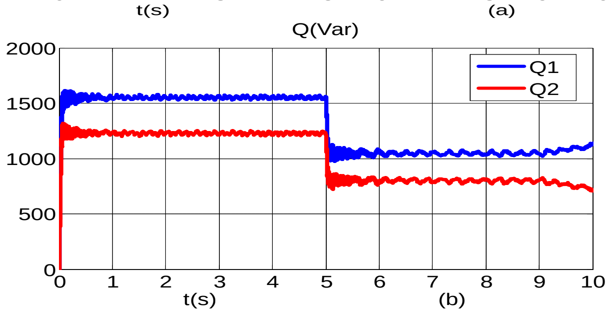

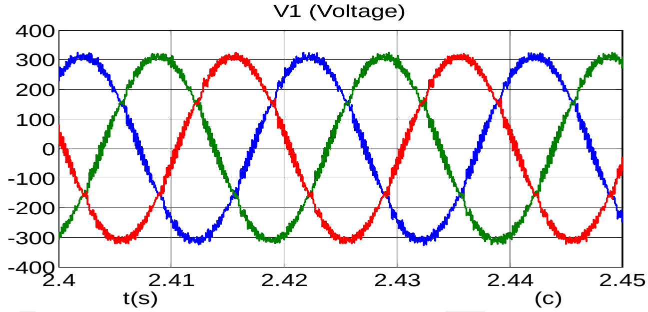

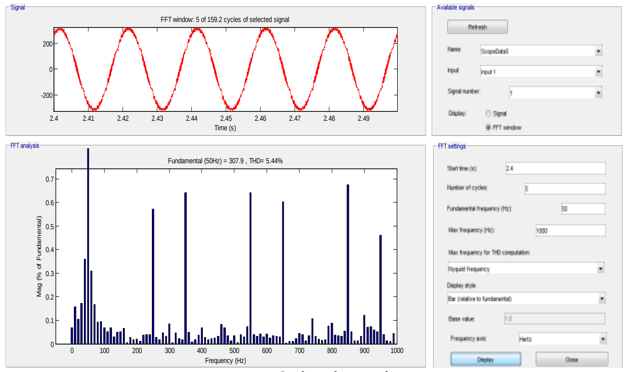

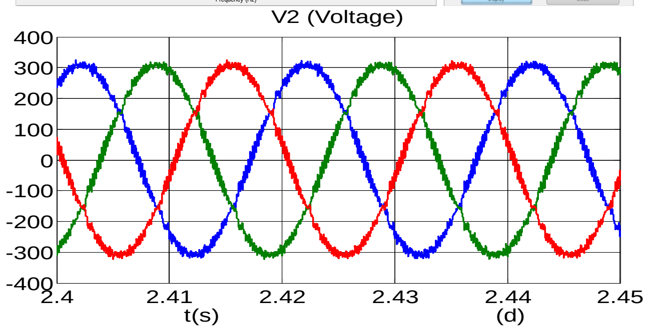

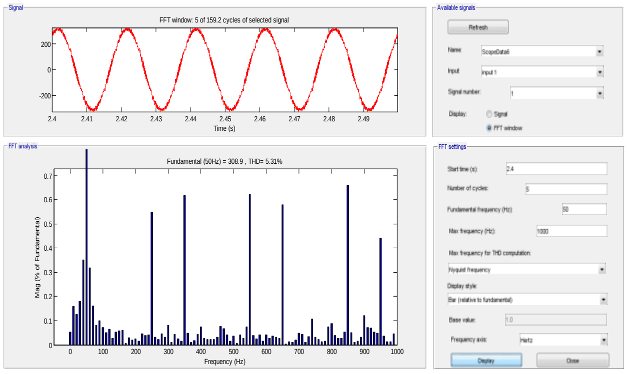

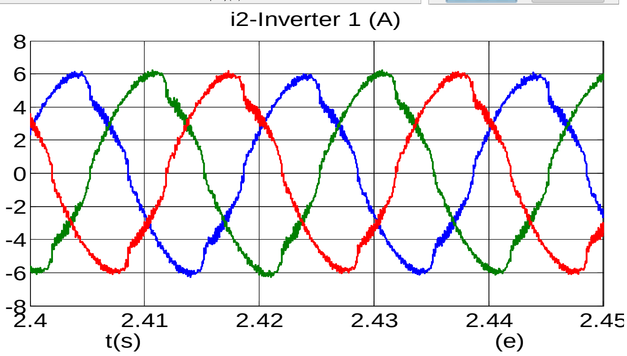

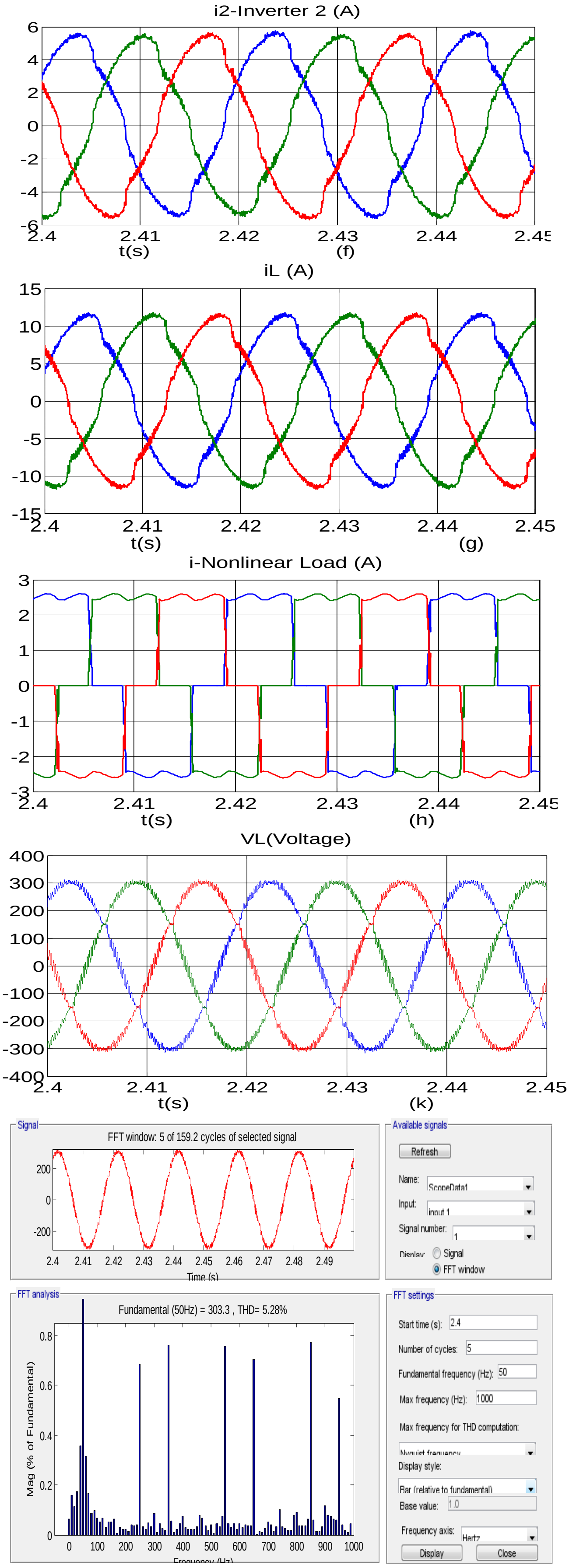

Figure 14: Simulation results with traditional droop control method, (a)Active power sharing, (b) Reactive power sharing, (c) Output voltages of inverter 1, (d) Output voltages of inverter 2, (e) Output currents of inverter 1, (f) Output currents of inverter2, (g) PCC currents, (h) Nonlinear load currents, (k) PCC voltages

Figure 14 shows the simulation results when the conventional droop control is applied with the power sharing ratio of 1:1. In case of the two line impedances are difference, the active power sharing is equal to the ratio of 1:1 by the conventional method as shown in Fig. 14a. However, the reactive power sharing is not good with the ratio of 1:1 as shown in Fig. 14b, in case of the two line impedances are different as shown in Table II. The conventional method cannot be applied to the power sharing when the line impedances are different and microgrid has nonlinear load and unbalane load.

The three-phase voltage and current waveforms of the output inverter 1, inverter 2 and PCC using the traditional droop control method are shown in Figure 14(c); 14(d); 14(e); 14(g) and 14(k).

From Figure 14(e) and 14(f), they are clearly shown that the current outputs of the inverter 1 and inverter 2 are difference, in case of the two line impedances are different.

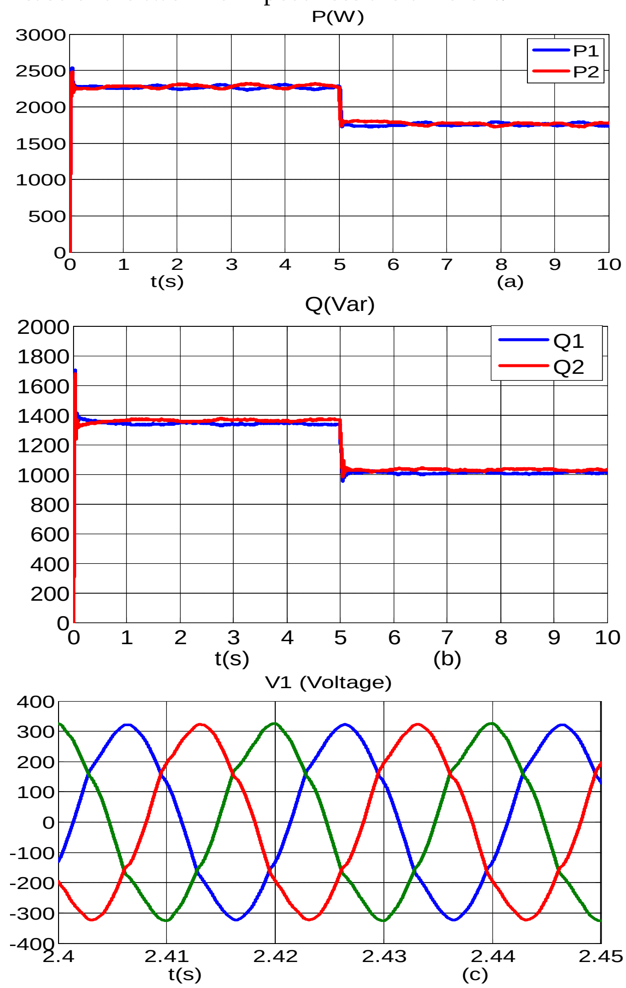

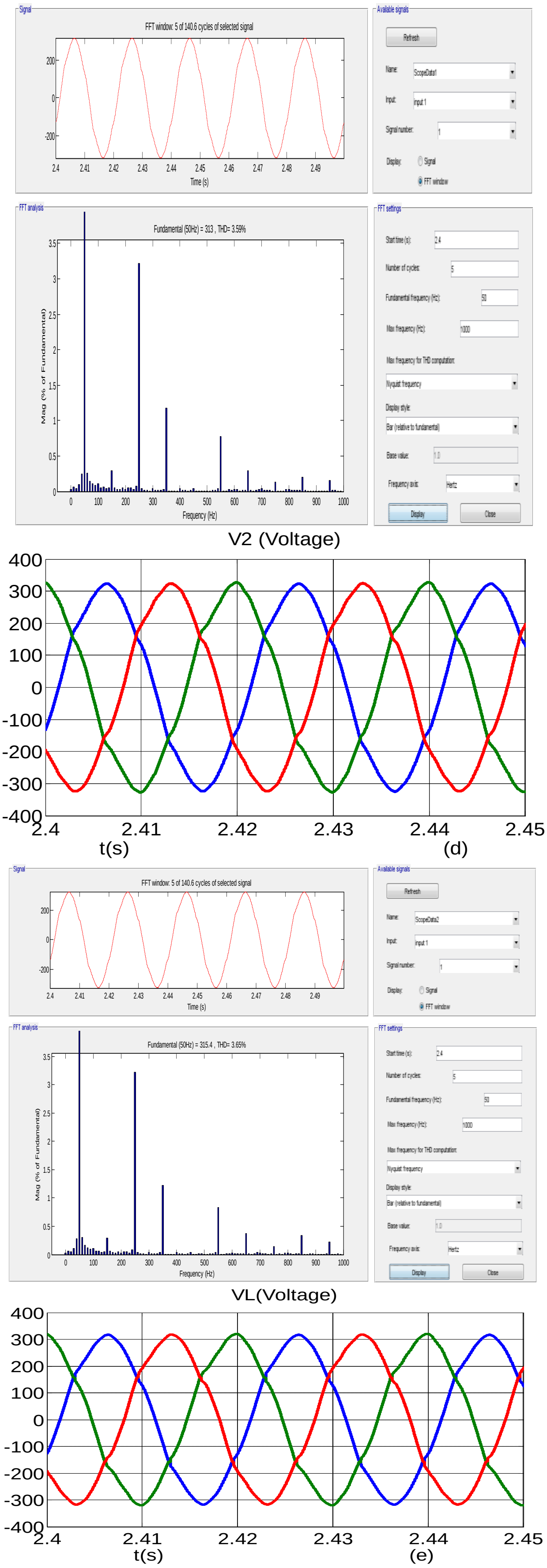

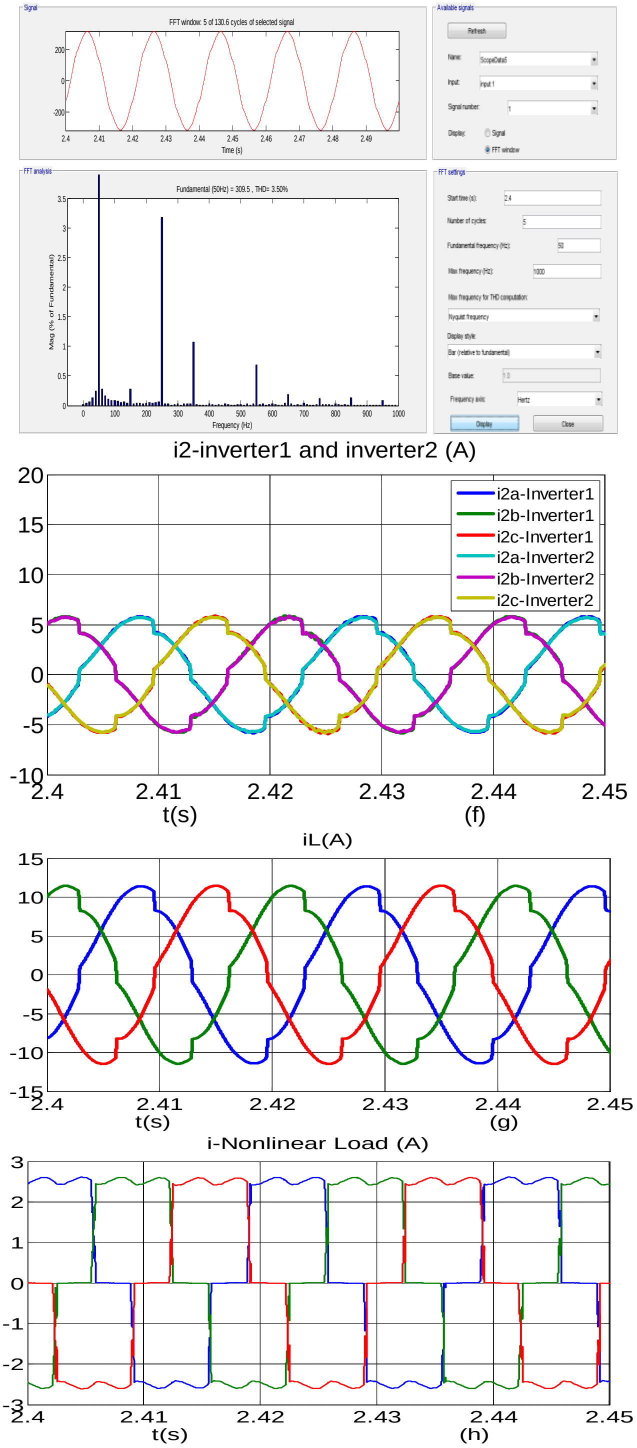

Figure 15: Simulation results with proposed control method, (a)Active power sharing, (b) Reactive power sharing, (c) Output voltages of inverter 1, (d) Output voltages of inverter 2, (e) PCC voltages (f) Output currents of inverter 1 and inverter 2, (g) PCC currents, (h) Nonlinear load currents

By using the proposed control strategy, the power sharing performance is improved as illustrated in Figure 15. From Figure 15(f), it is clearly shown that the current outputs of the inverter 1 and inverter 2 are same, and the current sharing errors are effectively decreased. As it can be seen, in Figure 15(a) and 15(b), the active and reactive power sharing are accurate with the proposed control method.

International Journal of Science and Research (IJSR)
ISSN: 2319-7064
ResearchGate Impact Factor (2018): 0.28 | SJIF (2018): 7.426

b) Simulation for power sharing of two identical inverters, the line impedances are difference, the loads are changed

In this case, the line parameters of the two inverters are given in Table III.

Table 3: Line Parameters of Two Inverters

Line parameters	Inverter 1	Inverter 2
Resistance R (Ω)	0.6	1.0
Inductance L (mH)	0.7	1.0

Parameters of linear load:

t=0-4s: P=2300W, Q=550Var, cosφ=0.9

t=4-8s: P=3400W, Q=2250Var, cosφ=0.83

t=8-12s: P=1000W, Q=900Var, cosφ=0.74

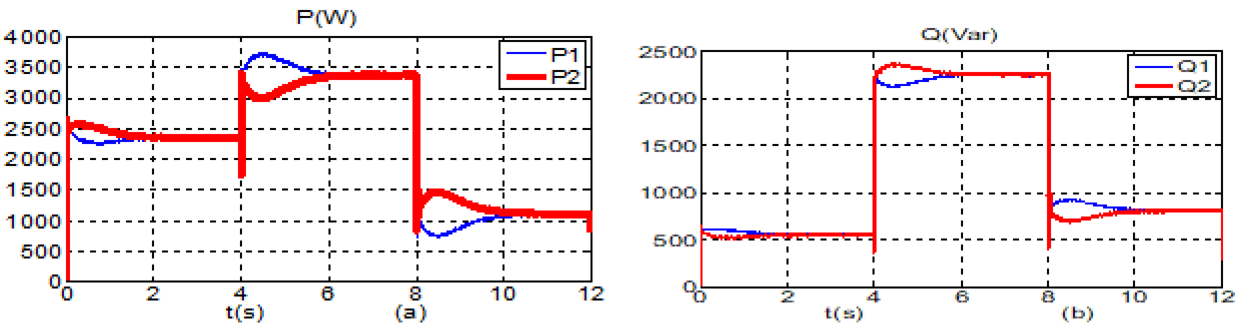

Figure 16: (a) Real power; (b) reactive power

Figure 16 shows that the proposed controller has result in good power sharing when the power of load varies.

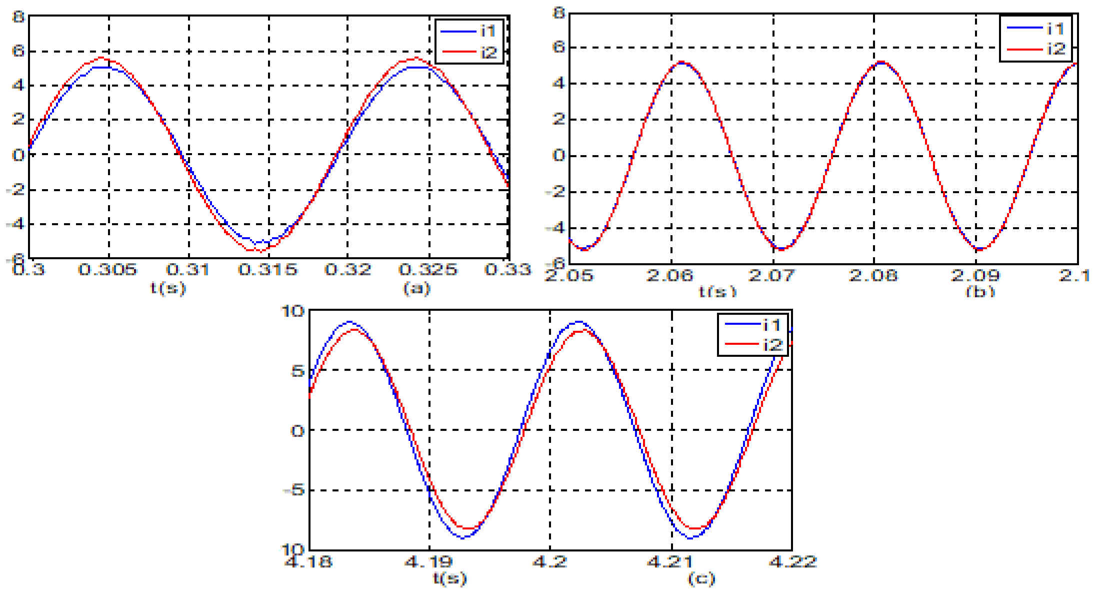

Figure 17: The current output of inverters

Figure 17(a) and 17(c) are shown response of phase current at output of inverter, we can see that during this time the controller has not reached the set state so there is a mismatch in the power sharing, so that the phase current is mismatch also. Figure 17(b) is shown the response of phase current in satablity, the current sharing is not mismatched.

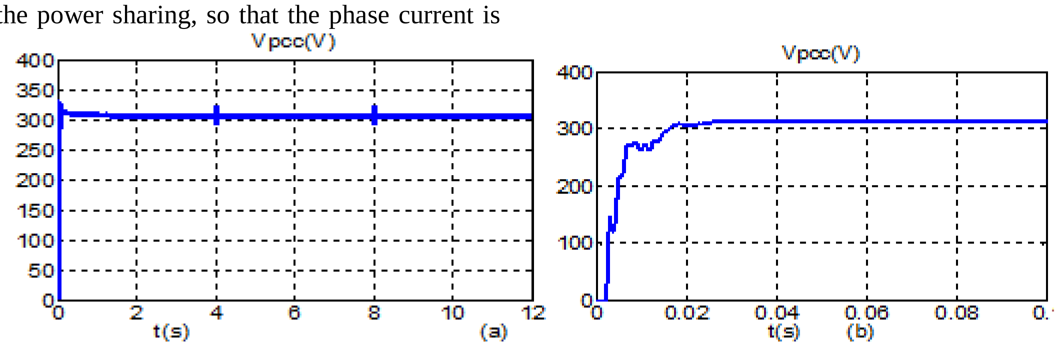

Figure 18: The voltage at PCC

Figure 18shows the voltage quality at the PCC, the voltage quality is always guaranteed by proposed controller.

c) Simulation for power sharing of two difference inverters (P1:P2=2:1), the line impedances are difference

In this case, the line parameters of the two inverters are given in Table IV.

Table 4: Line Parameters of Two Inverters

Line parameters	Inverter 1	Inverter 2
Resistance R (Ω)	0.4	0.8
Inductance L (mH)	0.6	1.0

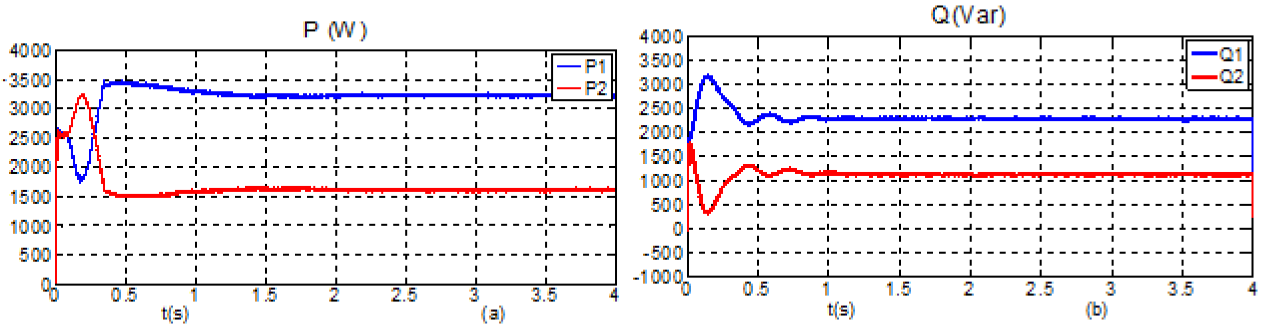

Figure 19: (a) Real power; (b) reactive power

From Fig. 19(a) and 19(b), it can be seen that the proposed control method provides a good power sharing. Figures 19 can shows accurate real and reactive power with a 2:1 ratio.

Total output power of each inverter:

$$P_1 = \frac{2}{3}\left(P_{local\ 1} + P_{local\ 2} + P_{public}\right) = \frac{2}{3}(700 + 760 + 3400) = 3240W$$

$$P_2 = \frac{1}{3}\left(P_{local\ 1} + P_{local\ 2} + P_{public}\right) = \frac{1}{3}(700 + 760 + 3400) = 1620W$$

$$Q_1 = \frac{2}{3}\left(Q_{local\ 1} + Q_{local\ 2} + Q_{public}\right) = \frac{2}{3}(500 + 700 + 2250) = 2300Var$$

$$Q_2 = \frac{1}{3}\left(Q_{local\ 1} + Q_{local\ 2} + Q_{public}\right) = \frac{1}{3}(500 + 700 + 2250) = 1150Var$$

d) Simulation for power sharing of three identical inverters (P1:P2:P3=1:1:1), the line impedances are difference

In this case, the line parameters of the three inverters are given in Table V.

Table 5: Line Parameters of Two Inverters

Line parameters	Inverter 1	Inverter 2	Inverter 3
Resistance R (Ω)	0.8	1.0	0.7
Inductance L (mH)	0.6	0.8	0.5

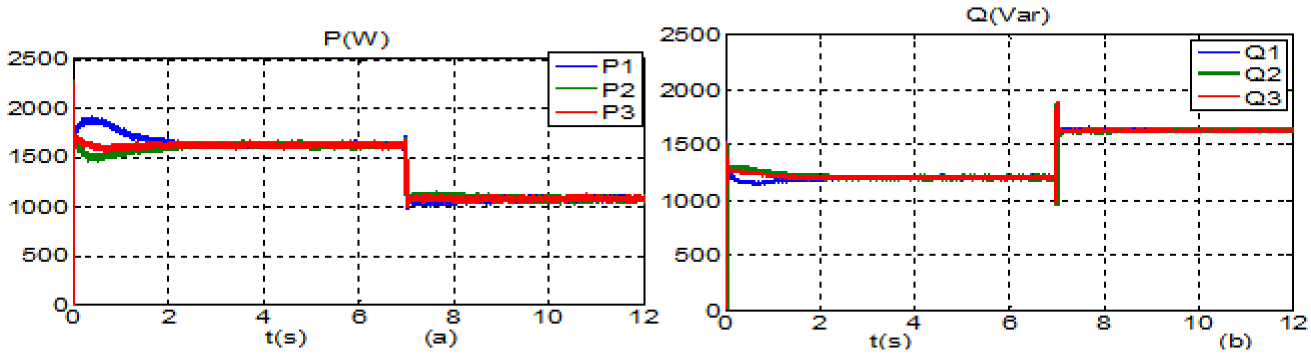

Figure 20: (a) Real power; (b) reactive power

Figure 20(a) and 20(b) can be seen that the proposed control method provides a good power sharing. Figures 20 can shows accurate real and reactive power with a 1:1:1 ratio.

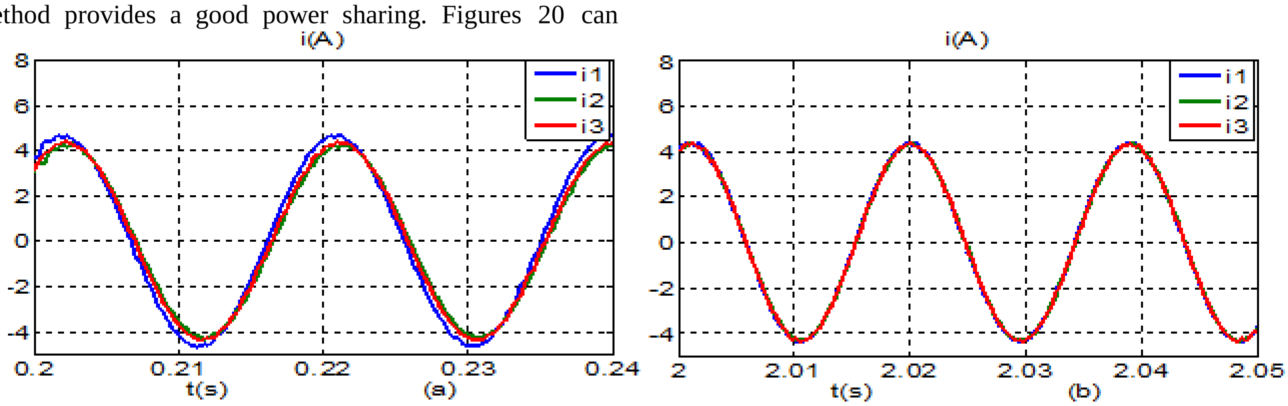

Figure 21: The current output of inverters

Figure 21(a) shows response of phase current at output of inverters, we can see that during this time the controller has not reached the set state so there is a mismatch in the power sharing, so that the phase current is mismatch also.

Figure 21(b) is shown the response of phase currents in satablity the current sharing is not mismatched.

e) Simulation for power sharing of two identical inverters, the line impedances are difference,the communication is interrupted

In this case, the line parameters of the two inverters are given in Table VI.

Table 6: Line Parameters of Two Inverters

Line parameters	Inverter 1	Inverter 2
Resistance *R* (Ω)	0.8	1.2
Inductance *L* (mH)	0.6	1.0

The communication is interrupted at t=3s and the communication is restored at t=8s, the load are changed in the period from t=5s to t=8s.

1) Simulation results with the proposed control

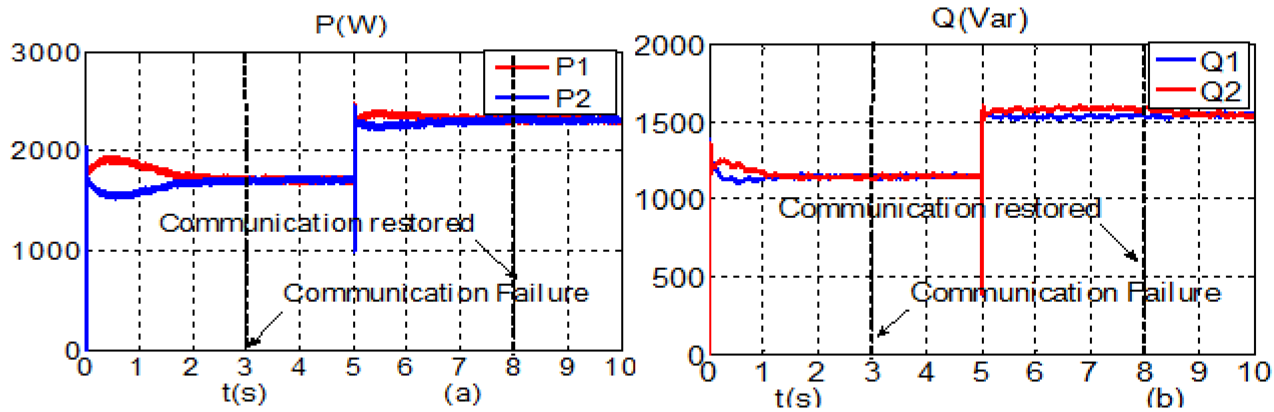

Figure 22: (a) Real power; (b) reactive power

2) Simulation results with the conventional droop control

In order to improve the performance of the reactive power sharing under the effect of the line impedance, some simulation tests have been carried out with the same scenario as in E1. However, the conventional droop control method is applied as shown in (5) and (6). The simulation results are shown in Fig. 23.

As shown in Figs. 23(a) and 23(b), the conventional method has a good performance for the case of line impedances that are identical. However, in the case of the line impedances are difference, as shown in Table VI, the reactive power sharing is not accurate. The line impedance does not have an effect on the active power sharing. However, the line impedance has an effect on the active power sharing.

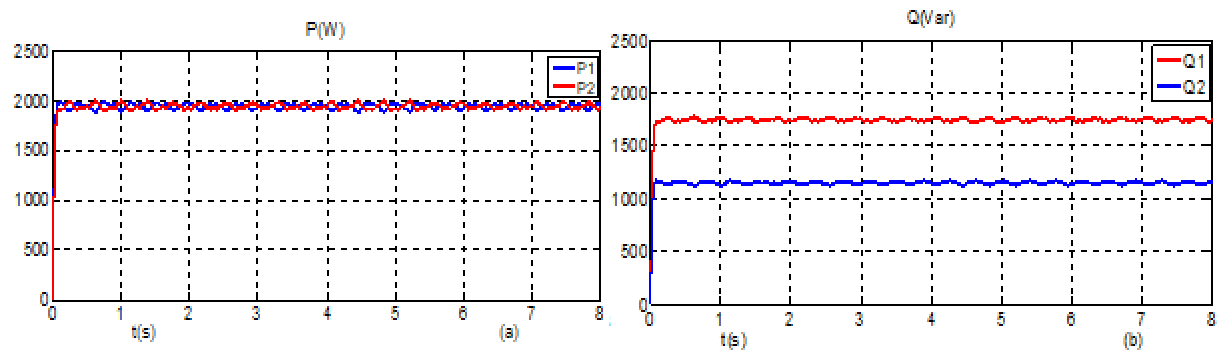

Figure 23: (a) Real power; (b) reactive power

Figure 22a, 22b show that in the period from 3s to 5s, although communication failure, but the load are not changed so the power sharing has been implemented correctly; in the period from 5s to 8s, the communication failure and the load are changed so the reactive power sharing hasn't been implemented correctly, but still better than the conventional droop controller in Figure 23b. The communication be restored after the 8s, so the power sharing has been implemented correctly.

f) Simulation in the case of the information update delay

The line parameters of the two inverters for this simulation are provided in Table VII.

Table 7: Line Parameters of Two Inverters

Line parameters	Inverter 1	Inverter 2
Resistance *R* (Ω)	0.8	1.2
Inductance *L* (mH)	0.6	1.0

The effect of time delays in communication is investigated by introducing a delay in the signal sent to proposed controller 1, not delay for proposed controller 2. In this case, the proposed controller 2 receives the Vpcc reference and starts acting before proposed controller 1. Which has more effect on the transients in comparison to the case when the delays are identical.The introduced time delay is chosen as 0.02s, which is significant given that the reference update period is 200µs. Simulation results are illustrated in Figure 24 and Figure 25.

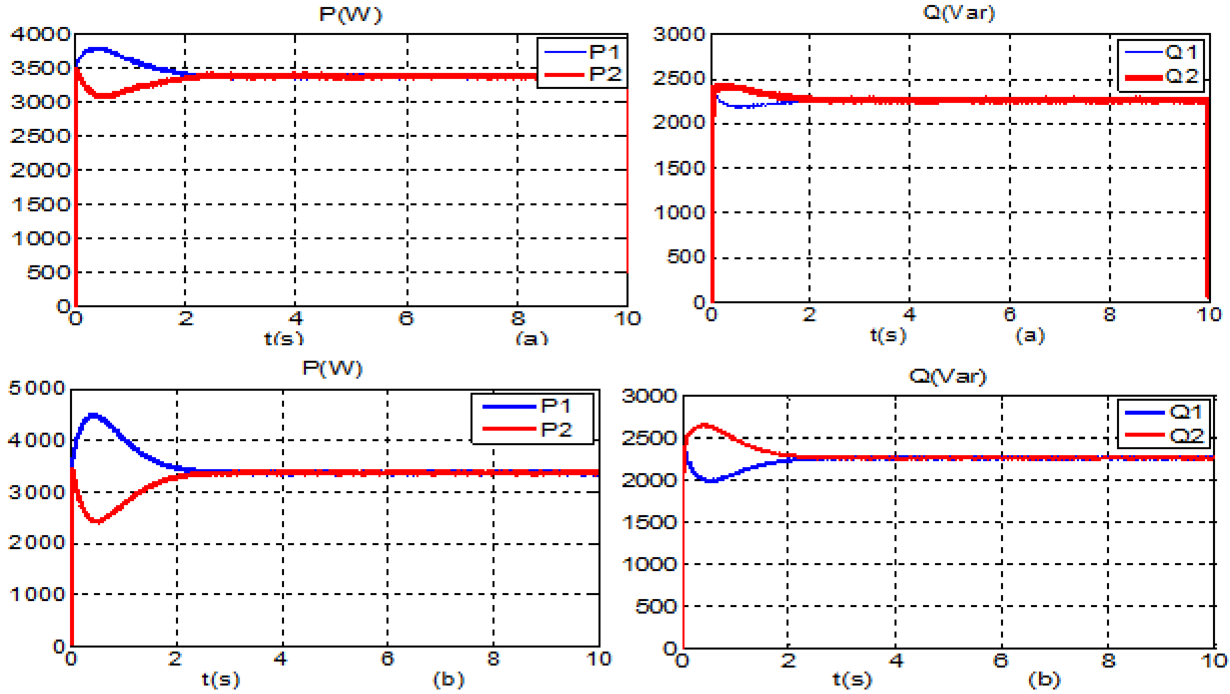

Figure 24: (a) Real power and reactive power when the proposed controller has not been delay; (b) Real power and reactive power when the proposed controller has been delay

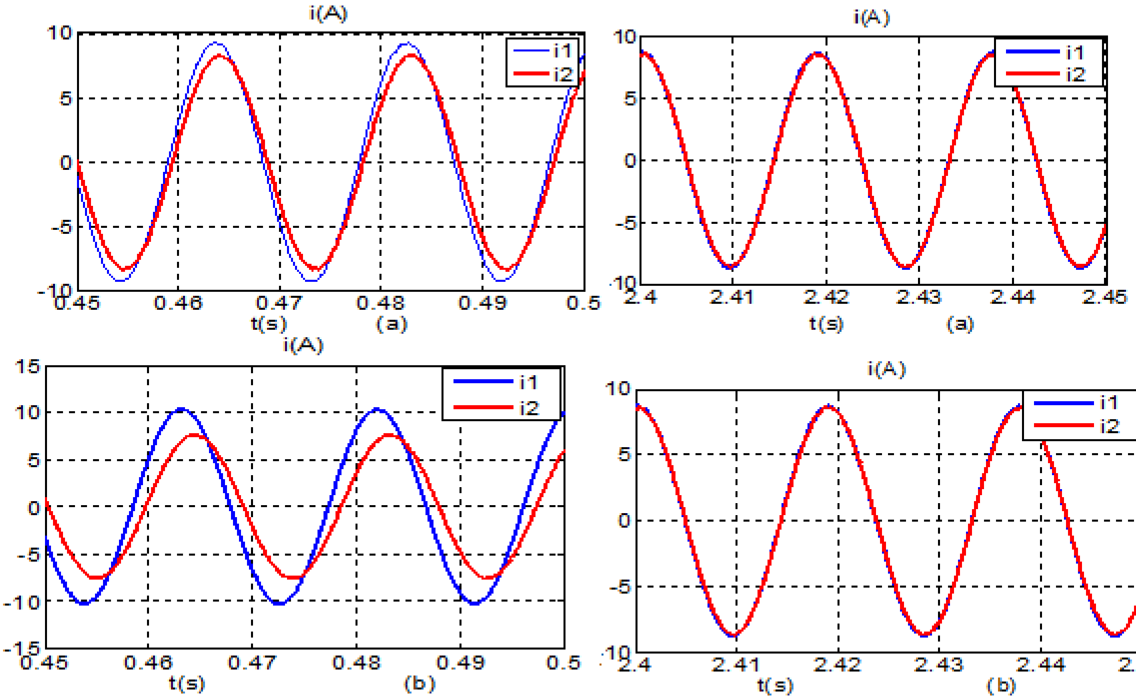

Figure 25: (a) Current output when the proposed controller has not been delay; (b) Current output when the proposed controller has been delay

The effect of time delays in communication is investigated by introducing a delay in the signal sent to proposed controller 2, not delay for proposed controller 1. The introduced time delay is chosen as 0.1s, a delay occurs at time t = 5s. Simulation results are illustrated in figure 26.

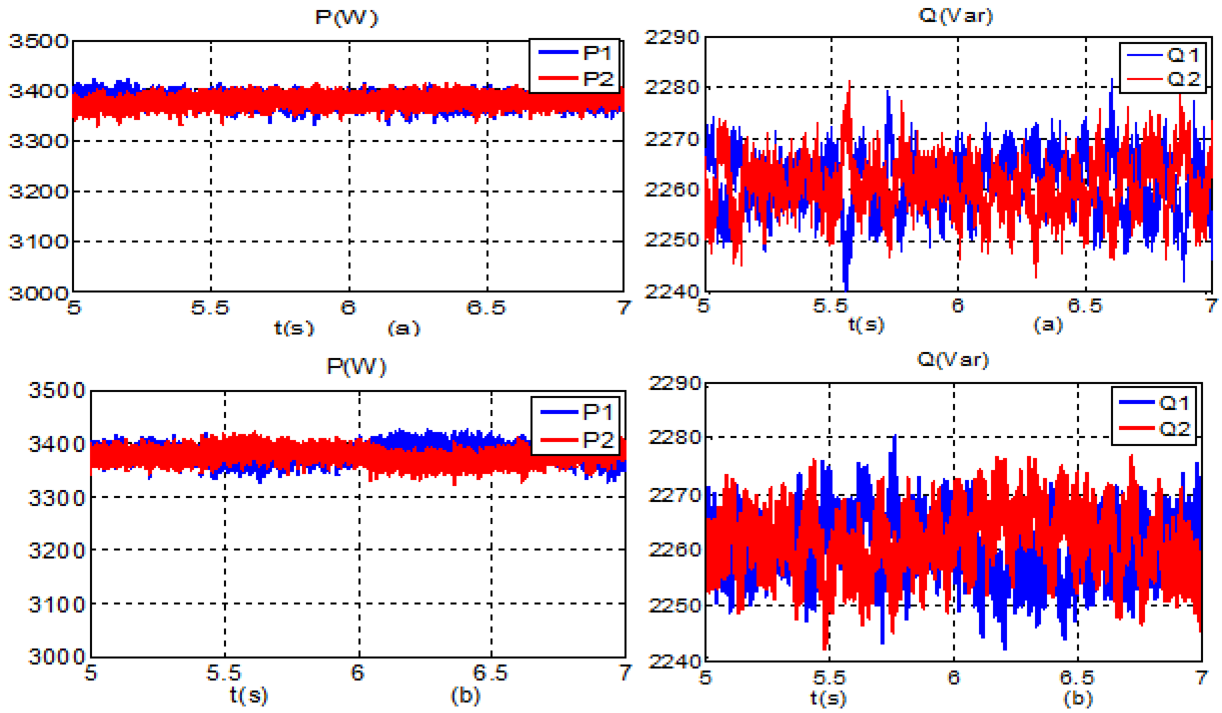

Figure 26: (a) Real power and reactive power when the proposed controller has not been delay; (b) Real power and reactive power when the proposed controller has been delay

Figure 24, 25, 26 shown that the time delay has little effect on the system transients. Most importantly, the time delay does not affect the accurate power sharing of the proposed controller. If delays occur in a steady state as Figure 26, it will not affect on the system transients.

4. Hardware Implementation Using a DSP

In this paper, a practical model has been developed for testing the proposed method. The developed hardware model consists of three 3-phase inverters, drivers of Semikron, LEM HX 20P and LV–25P are used as voltage and current sensors as shown in Figure 27. The proposed control method has been implemented on a TMS320F28335 DSP controller and the results obtained from the experiment have been captured by a Tektronix TDS2014B oscilloscope and a Fluke 345 PQ clamp meter. To maintain the load demand, the three inverters have been used with a parallel output connection while RS485 lines are used as a communication network. The experiment has been carried out on three test cases with different ratios for real and reactive powers. The results obtained from the experiment have verified the advantages of the proposed control method through case studies.

Figure 27: Hardware setup for the experiment

a) Case study 1: P1:P2 = 1:1, Q1:Q2 = 1:1, and the load changes

For this case, the ratio of the active and reactive power is 1:1 for the two inverters with a load fixed at a pre-determined value, the line impedances are difference. The measured power outputs for the twoinverters are shown in Figure 28 and 29. The loads are changed from 925 W to 1250W and 350Var to 520Var. The power sharing errors for this case are very small.

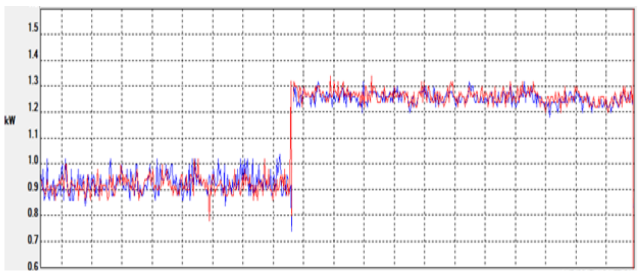

Figure 28: Real power sharing

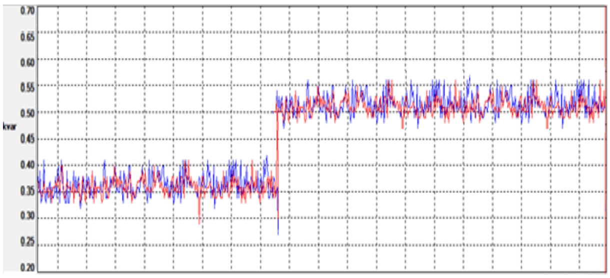

Figure 29: Reactive power sharing

b) Case study 2: P1:P2:P3 = 1:1:3, and the load changes

This case corresponds to the ratio of the active powers being 1:1:3 and load changes with steps within pre-determined limits. The measured active power outputs for the three inverters are shown in Figure 30. The obtained active power outputs for the three inverters increase within the limits as P_{1min} = 480W, P_{2min} = 480W and P_{3min} = 1450WP_{1max} = 750W, P_{2max} = 750 W, P_{3max} = 2250 W. These results have demonstrated the response capability of the system based on the new control strategy when the load continuously changes online with a constant ratio. The active power sharing errors for this case are very small.

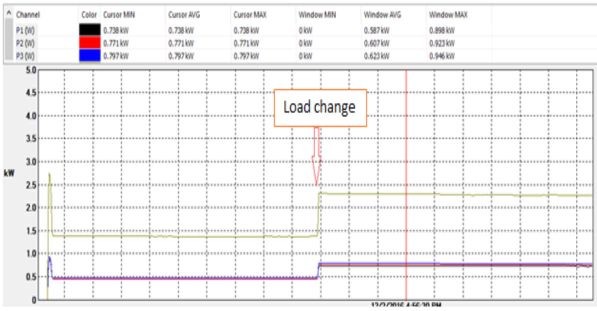

Figure 30: Real power sharing

c) Case study 3: P1:P2:P3 = 1:1:1, Q1:Q2:Q3 = 1:1:1, and the load changes

Fig. 31 shows the active and reactive powers of the three inverters in case of load changes. It can be seen that the ratio of the active and reactive powers is still kept at 1:1:1 when the load increases and decreases.

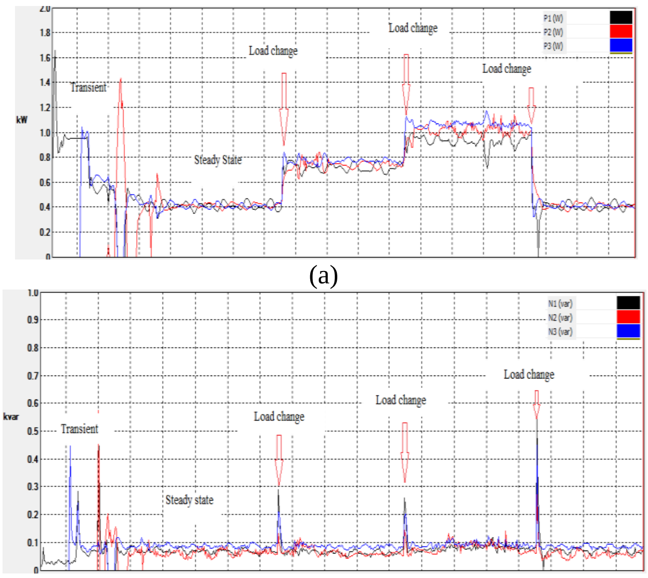

(a)

(b)

Figure 31: (a) Real power; (b) reactive power

5. Conclusion

This paper has proposed a new method for an accurate load sharing ratio between the paralleled inverters in islanded microgrids. In this study, the voltage droop slope is tuned to compensate for the mismatch in the voltage drops across line impedances by using communication links. The method will ensure in accurate power sharing even if the communication is interrupted. If the load changes while the communication is interrupted, the accuracy of power sharing is reduced but the proposed method is better than the conventional droop control method. In addition, the accuracy of power sharing base on the proposed method is not affected by the time delay in the communication channel and local loads. Simulation results in Matlab/Simulink and hardware experiments have demonstrated the superiority of the proposed strategy in any case with any ratio.

References

[1] Hua Han, XiaochaoHou, Jian Yang, Jifa Wu, Mei Su, and Josep M. Guerrero, "Review of Power Sharing Control Strategies for Islanding Operation of AC Microgrids," *IEEE Trans. Smart Grid*, Vol. 7, No. 1, pp. 200-216, Jan. 2016.

[2] J. Rocabert, A. Luna, F. Blaabjerg, and P. Rodriguez, "Control of power converters in AC microgrids," *IEEE Trans. Power Electron*., Vol. 27, No. 11, pp. 4734-4739 Nov. 2012.

[3] Q.-C. Zhong. "Robust Droop Controller for Accurate Proportional Load Sharing Among Inverters Operated in Parallel". *IEEE Trans. Power Electron*., Vol. 60,No. 4, pp. 1281-1291, Apr. 2013.

[4] [141] MdAlamgirHossain ,Hemanshu Roy Pota, WalidIssa and Md Jahangir Hossain "Overview of AC Microgrid Controls with Inverter-Interfaced Generations", Energies, 30 August 2017.

[5] S. V. Iyer, M. N. Belur, and M. C. Chandorkar, "A generalized computational method to determine stability of a multi-inverter microgrid," *IEEE Trans. Power Electron.*, Vol. 25, No. 9, pp. 2420-2432, Sept. 2010.

[6] J. Justo, F. Mwasilu, and J. Lee, "AC microgrids versus DC microgrids with distributed energy resources: A review," *Renew. Sustain. Energy Rev.*, Vol. 24, pp. 387-405, 2013.

[7] J. Hu, J. Zhu, D. G. Dorrell, and J. M. Guerrero, "Virtual flux droop method - A new control strategy of inverters in microgrids," *IEEE Trans. Power Electron.*, Vol. 29, No. 9, pp. 4704-4711, Sept. 2014.

[8] J. M. Guerrero, J. C. Vasquez, J. Matas, L. G. de Vicuna, and M. Castilla, "Hierarchical control of droop-controlled ac and dc microgrids - A general approach towards standardization," *IEEE Trans. Ind. Electron.*, Vol. 58, No. 1, pp. 158-172, Jan. 2011.

[9] J. C. Vasquez, J. M. Guerrero, M. Savaghebi, J. Eloy-Garcia, and R. Teodorescu, "Modeling, analysis, and design of stationary-reference frame droop-controlled parallel three-phase voltage source inverters," *IEEE Trans. Ind. Electron.*, Vol. 60, No. 4, pp. 1271-1280, Apr. 2013.

[10] M. Savaghebi, A. Jalilian, J. C. Vasquez, and J. M. Guerrero, "Secondary control scheme for voltage

unbalanced compensation in an islanded droop controlled microgrid," *IEEE Trans. Smart Grid*, Vol. 3, No. 2, pp. 797-807, May 2012.

[11] M. A. Abusara, J. M. Guerrero, and S. M. Sharkh, "Line-interactive ups for microgrids," *IEEE Trans. Ind. Electron.*, Vol. 61, No. 3, pp. 1292-1300, Mar. 2014.

[12] H. Mahmood, D. Michaelson, and J. Jiang, "Accurate reactive power sharing in an islanded microgrid using adaptive virtual impedances," *IEEE Trans. Power Electron.*, Vol. 30, No. 3, pp. 1605-1617, Mar. 2014.

[13] J. He, Y. W. Li, J. M. Guerrero, J. C. Vasquez, and F. Blaabjerg, "An islanded microgrid reactive power sharing scheme enhanced by programmed virtual impedances," *in Proc. IEEE Int. Symp. Power Electron. Distrib. Gener. Syst.* 2012, pp. 229-235.

[14] J. He, Y. W. Li, J. M. Guerrero, F. Blaabjerg, and J. C. Vasquez, "An islanding microgrid power sharing approach using enhanced virtual impedance control scheme," *IEEE Trans. Power Electron.*, Vol. 28, No. 11, pp. 5272-5282, Nov. 2013.

[15] K.S.Rangasamy College of Technology K.S.Rangasamy College of Technology Tiruchengode, Tamil Nadu, India Tiruchengode, Tamil Nadu, India, S.S. Balasreedharan, PG Student S. Thangavel, Professor Department of Electrical and Electronics Engineering, "India an adaptive fault entification scheme for DC Microgrid using event based classification", Systems, Jan. 22 – 23, 2016.

[16] Mr.V.Prasad, M.Tech, M.I.M.E.S Assistant Professor, Department of ECE, Shree Institute of Technical Education,Renigunta, Tirupati, "A Wireless Communication System for Data Transfer within Future Micro grids", International Journal &Magazine of engineering, Vol, No.3 (2016).

[17] M. Farhadi, Student Member, IEEE and O. A. Mohammed, Fellow, IEEE Energy Systems Research Laboratory, Department of Electrical and Computer Engineering Florida International University Miami, Florida, USA, "A New Protection Scheme for Multi-Bus DC Power Systems Using an Event Classification Approach", 2015, IEEE.

[18] Mahdi Ashabani, Yasser A.-R. I. Mohamed, *Senior Member*, *IEEE*, MojtabaMirsalim, *Senior Member*, *IEEE*, and Mohammad Aghashabani, "Multivariable Droop Control of Synchronous Current Converters in Weak Grids/Microgrids With Decoupled *dq*-Axes Currents", IEEE Transaction on Smart grid, Vol. 6, No. 4, 2015.

[19] M.S. Hamad, M.I. Masoud, B.W. Williams, "Medium-voltage 12-pulseconverter: output voltage harmonic compensation using a series APF", IEEETrans. Ind. Electron. 61 (1) (2014) 43–52.

[20] A. Chandra, B. Singh, B. Singh, K. Al-Haddad, "An improved control algorithm ofshunt active filter for voltage regulation, harmonic elimination, power-factor correction, and balancing of nonlinear loads", IEEE Trans. Power Electron. 15(3) (2000) 495–507.

[21] P. Rodriguez, A. Luna, M. Ciobotaru, R. Teodorescu, F. Blaabjerg, "Advanced gridsynchronization system for power converters under unbalanced anddistorted operating conditions", IECON 2006-32nd Annual Conference on IEEEIndustrial Electronics (2006) 5173–5178, IEEE.

[22] A. Garcia-Cerrada, O. Pinzon-Ardila, V. Feliu-Batlle, P. Roncero-Sánchez, P.García-González, "Application of a repetitive controller for a three-phaseactive power filter", IEEE Trans. Power Electron. 22 (1) (2007) 237–246.

[23] R. Ghanizadeh, M. Ebadian, G.B. Gharehpetian, "Non-linear load sharing andvoltage harmonics compensation in islanded microgrids with converterinterfaced units", Int. Trans. Electr. Energy Syst. 27 (1) (2016).

[24] M. Savaghebi, A. Jalilian, J.C. Vasquez, J.M. Guerrero, "Secondary control forvoltage quality enhancement in microgrids", IEEE Trans. Smart Grid 3 (4)(2012) 1893–1902.

[25] X. Wang, F. Blaabjerg, Z. Chen, "Autonomous control of inverter-interfaceddistributed generation units for harmonic current filtering and resonancedamping in an islanded microgrid", IEEE Trans. Ind. Appl. 50 (1) (2014)
452–461.

[26] L. Yun Wei, K. Ching-Nan, "An accurate power control strategy forpower-electronics-interfaced distributed generation units operating in alow-voltage multibusmicrogrid", IEEE Trans. Power Electron. 24 (12) (2009)2977–2988.